Cavity Phase Matching via an Optical Parametric Oscillator Consisting of a Dielectric Nonlinear Crystal Sheet

Z. D. Xie,* X. J. Lv, Y. H. Liu, W. Ling, Z. L. Wang, Y. X. Fan, and S. N. Zhu†

National Laboratory of Solid State Microstructures and Department of Physics, Nanjing University, Nanjing 210093, China
(Received 29 November 2010; published 22 February 2011)

We experimentally demonstrate cavity phase matching for the first time using a sheet optical parametric oscillator which is made of an x-cut KTiOPO$_4$ crystal sheet. This microcavity presents 220 kW peak power capability for near-frequency-degenerate parametric outputs with up to 23.8% slope efficiency. It also features unique spectral characteristics such as single-longitudinal-mode and narrow linewidth. These attractive properties predict broad applications of such a mini-device, such as terahertz generation, photonic integration, spectroscopy, and quantum information, etc.

In the recent years, optical microcavities have received considerable attention as integrated light sources and devices for the future applications in optical sensing, computing, and communication. The wave-guide-style microcavities, especially the whispering-gallery-mode microcavities are attractive due to their ultrahigh optical quality factors Q and thereby the unique spectral features. They not only work as laser active devices such as the microdisk laser [1], but also have been demonstrated to be useful for parametric processes, for example, second-harmonic generation [2–4], tunable frequency comb generation [5], parametric oscillation [6–8], and Raman lasing [9], etc. On the other hand, as proven by the fast-developing vertical-cavity surface-emitting lasers, the Fabry-Perot microcavities (FPMCs) have great advantages for high-power operation, while at the same time maintaining good beam qualities. Despite the lack of experimental realizations, theoretical studies [10–12] have shown potential applications of FPMC in nonlinear optics, which can be dated back to the early work by Armstrong *et al.* in 1962 [13]. Among these studies, the subcoherence length FPMC is of special interest, where the resonance also serves to compensate for the phase mismatching and efficient frequency conversion is expected. The principle of this so-called cavity phase matching (CPM) can be interpreted in comparison with the well-known quasi–phase-matching (QPM) method [14–18]. As shown in Fig. 1(a), QPM requires engineering microstructure inside the nonlinear medium to compensate the phase mismatch by reversing orientation of the nonlinear polarization; while in the case of CPM, the resonance recirculation in cavity can ensure that the traveling light and reflected light are exactly in phase in every circling. This is equivalent to extend the effective nonlinear interaction path, and therefore, increase the frequency conversion efficiency by a factor of Q [13].

In this Letter, we revisit the concept of CPM, and have realized it experimentally for the first time, by using a sheet optical parametric oscillator (SOPO). The SOPO consists of a dielectric nonlinear crystal sheet, whose two end-faces are high-reflectance coated, forming a high-Q FPMC that can provide double resonances for both signal and idler. Although the thickness of the sheet is less than one coherence length, such a sheet oscillator exhibits high slope efficiency and peak power output, as well as near-transform-limited spectral and near-diffraction-limited spatial features. These novel features are of wide interest in the nonlinear optics, laser physics, and optical technology communities.

Similar to the case of QPM, the CPM allows a certain amount of phase mismatch, and therefore it is necessary to introduce an effective nonlinear coefficient d_{eff} to describe the strength of the nonlinear coupling, instead of the nonlinear coefficient d of the material. As shown in Fig. 2, d_{eff} can be expressed in the form of the following sinc function:

$$d_{\text{eff}} = d \left| \text{sinc}\left(\frac{\pi l_{\text{cav}}}{2 l_{\text{coh}}}\right) \right|, \tag{1}$$

where [13,19]

$$l_{\text{coh}} = \pi/(k_p - k_s - k_i) \tag{2}$$

and l_{cav} is the cavity length; $\vec{k}_p$, $\vec{k}_s$, and $\vec{k}_i$ are the wave vectors of pump, signal, and idler, respectively.

The most efficient CPM is achieved when $l_{\text{cav}} \leq l_{\text{coh}}$, otherwise destructive interference occurs and d_{eff} drops significantly. When l_{cav} is around odd times of l_{coh}, the high order CPM takes place, however, with smaller d_{eff}. In our study, we always keep $l_{\text{cav}} \leq l_{\text{coh}}$, i.e., the first-order CPM.

For the x-cut KTiOPO$_4$ (KTP) crystal, we choose type-II matching for the OPO system, where the idler has the same polarization as the pump along the y axis, while the signal beam has an orthogonal polarization along the z axis. The SOPO we use is fabricated from a monolithic crystal after fine polishing, down to 217 μm in thickness and with the surface area of 2 mm $\times$ 2 mm in the yz plane. The two end faces of the crystal sheet are both antireflection coated
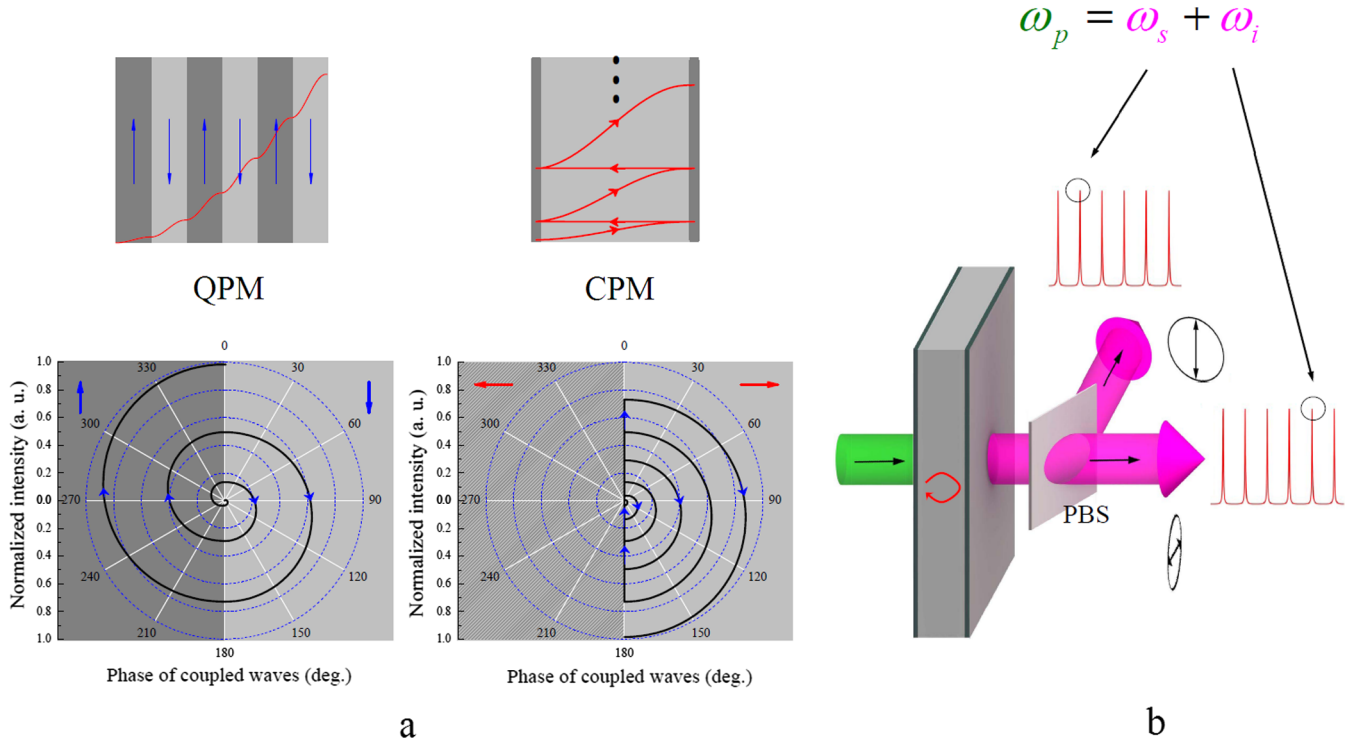
FIG. 1 (color online).   (a) The normalized intensity of the converted light as a function of the phase of the three coupled light waves in a QPM material (left) and a sheet nonlinear cavity (right). In QPM material, the nonlinear polarization of the crystal is reversed every coherence length, and therefore, the light waves always have the correct phase for nonlinear amplification. The phase correction is also the key issue for CPM; however, it is achieved by the total reflection on the cavity mirrors. (b) In the case of type-II optical parametric oscillation, the reflection circulation in the CPM also requires a cavity mode matching for signal and idler with the incidence pump. Only one pair of the signal and idler modes can be excited simultaneously in this study, which ensures single-longitudinal-mode oscillation.

for 532 nm (reflectivity $R < 1\%$), and high-reflection coated ranging from 1000 to 1100 nm with $R > 99.8\%$ for the input surface and $R = 98.2\%$ for the output surface, respectively. The SOPO shows a high Q value up to 1.6×10^5 (or a finesse F of 292) for signal or idler in terms of the measurement, which means the 217 μm thick crystal sheet due to the resonance in cavity has an equivalent interaction length of $l_{\mathrm{Equ}} = 63$ mm.

Considering the dispersion of x-cut KTP crystal [20], the first-order CPM allows large bandwidths of the signal and idler beams at 532 nm pump, which corresponds to a tunable signal output with a wavelength range from 1016.4 to 1069.4 nm. Meanwhile, a noncritical phase matching occurs:

$$532 \text{ nm (pump)} \rightarrow 1041.4 \text{ nm (signal)}$$
$$+ 1087.6 \text{ nm (idler).} \quad (3)$$

This indicates the coherence length $l_{\mathrm{coh}} \rightarrow \infty$, and the phase matching is always satisfied at the point. As deviating from this point, the CPM plays a particular role in extending the bandwidth of the noncritical phase matching and making an effective interaction length F times of l_{cav}.

In our experiment, the SOPO was pumped by a single-longitudinal-mode frequency-doubled yttrium-aluminum-garnet laser, which was the pump source of a commercial tunable OPO system (Sunlite, Continuum, Santa Clara, CA), with pulse duration of 5 ns and repetition rate of 10 Hz. The pump beam was first focused onto a small pinhole for selecting TEM_{00} mode, and then imaged onto the SOPO. The SOPO worked in a temperature-controllable oven with an accuracy of 0.01 °C. The doubly resonance configuration required precise longitudinal mode matching for signal and idler simultaneously [Fig. 1(b)]. When a proper temperature was set, the signal and idler beams could be generated in pairs with near TEM_{00} mode. As shown in Fig. 3, the spectra of the signal and idler captured by a spectral meter presented a single-longitudinal-mode oscillation. Since the resolution of spectra were limited by the spectra meter to about 60 GHz, which is sufficient to resolve the longitudinal mode spacing (~ 390 GHz) of the SOPO but not enough to measure the linewidth of the outputs, we had to do further measurement of the signal (or idler) using a Mach-Zehnder interferometer. The interference visibility was recorded by changing the relative time delay between the two arms. As shown in Fig. 3(b), the linewidth of the signal (or idler) was around
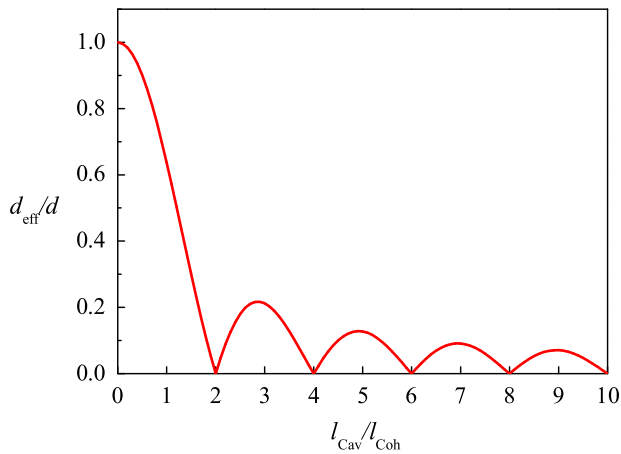
FIG. 2 (color online). When $l_{cav} \lesssim l_{coh}$, unidirectional conversion is ensured which yields to a higher d_{eff} than the first-order QPM. When l_{cav} is even times of l_{coh}, a complete destructive interference occur and $d_{eff} = 0$. When l_{cav} approaches odd times of l_{coh}, d_{eff} reaches peak value which may be used for high order CPM.

440 MHz, indicating the output pulses were nearly transform limited. This is very important for spectroscopic applications.

Interestingly, the signal and idler were tuned in a quasi-continuous way by changing operating temperature or pump wavelength. The longitudinal mode hopping occurred when the operating temperature changed around every 2.5 °C. The hopping originated from the doubly resonance configuration of the cavity as discussed previously. The experimental data exhibited a 47.8 nm tuning range (for signal) when the operating temperature varied from 32.00 to 115.60 °C [Fig. 4(a)]. This tuning corresponded to a coherence length change from $1.02l_{cav}$ to $96.8l_{cav}$, which was covered by the first-order CPM. The tuning was achieved by the change of pump wavelength as well. The tunable pump beam was provided by the output of the Sunlite OPO system. This pump had a pulse width of 4 ns, a repatriation rate of 10 Hz and a narrow linewidth of less than 0.075 cm^{-1} ($\sim$ 2.2 GHz), which was comparable with the FWHM of the transmission peaks of the sheet cavity. As shown in Fig. 4(b), broad tuning up to 38.8 nm for the signal was achieved while the pump's wavelength only changed 0.45 nm. Many diode lasers can be tuned in such a narrow range and may be used as a pump for such a compact tunable SOPO device.

We measured the output power dependence on the pump at the operating temperature of 54.00 °C, when the signal and idler located at 1028.14 and 1103.10 nm, respectively. The corresponding $l_{coh} = 1.98l_{cav}$, i.e., $d_{eff} = 0.9d$, according to Eq. (1). As shown in Fig. 5(a), the oscillation started with a threshold of about 50 μJ and the total output (signal and idler) exceeded 51 μJ at the pump of 295 μJ, with a peak conversion efficiency of 18.6%. The measured slope efficiency was around 21.2%. Considering the 10%
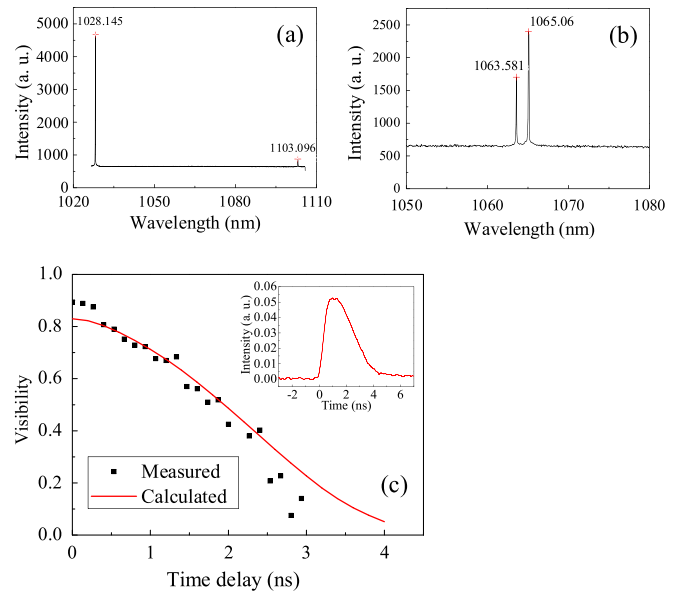

FIG. 3 (color online). Captured spectra of signal and idler beams at $t = 54.00$ °C (a) and $t = 113.50$ °C (b). The low strength of signal at 1100 nm originates from the lower efficiency of the silicon CCD of spectral meter at this wavelength. (c) The visibility of interference as a function of the relative time delay of two arms of the interferometer. The solid curve is the Fourier transform of captured pulse waveform (see insertion). It fits well with the measured data which show the signal light is nearly transform-limited.

loss of the high-pass filters placed in front of the detectors to block the pump light, the actual conversion efficiency and slope efficiency can be calibrated to be 21.7% and 23.6%, respectively. In the above measurement the waist of pump beam was 300 μm, and an actual output energy density of 72 mJ/cm^2 was achieved from this thin sheet. Enlarging the optical aperture can result in further increase of the output power. We increased the beam size to 1.3 mm in the following measurement. The total output of signal and idler raised up to a maximum of 778 μJ, which corresponded to a peak power of 220 kW [Fig. 5(b)]. The conversion efficiency was still as high as 17.3% at 4.5 mJ
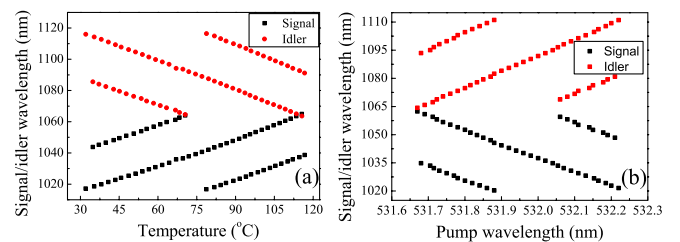

FIG. 4 (color online). Wavelengths of signal and idler lights as a function of temperature (a) or the pump wavelength (b). It worth noting that there is only one pair of signal and idler beams at one temperature or pump wavelength because of the small bandwidth of the longitudinal mode matching, although the matching conditions seem to be close in the above figures.
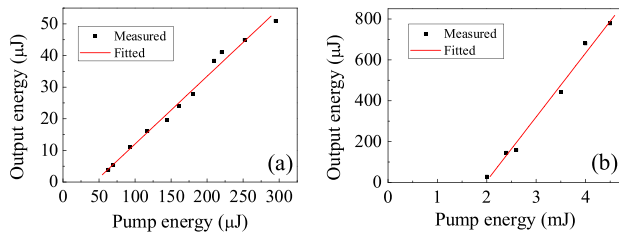
FIG. 5 (color online). Output pulse energy of both signal and idler light as a function of pump pulse energy with pump light waist of 300 μm (a) or 1.3 mm (b).

pump energy without noticeable damage to this SOPO. The sub-milli-joule level output was sufficient for the study of nonlinear effects in a number of different applications, and watt-level average power could be expected if using a quasicontinuous laser pump for such a SOPO. We noticed slight drop in the efficiency and beam quality for the large pump beam size, which was caused by the imperfection on the cavity surfaces. By improving the polishing quality, higher efficiency and better beam quality can be achieved, and the output power is scalable by further enlarging the surface area of the SOPO.

Like the conventional QPM method, the CPM extends the equivalent interaction length of the nonlinear interaction without the requirement of nature phase matching, and is universal to realize phase matching for the entire transparent range for the nonlinear medium. Moreover, the SOPO does not need the poling technique which is usually tricky for fabricating the QPM materials, which means it is applicable to nonferroelectric crystals, such as the famous BBO, LBO, etc.; a large optical aperture is easy to be achieved which allows considerable power output from such a monolithic microcavity. In this work, we have shown an example of SOPO with submillimeter thickness, where a small dispersion of the nonlinear crystal is required to provide a relatively long coherence length. However, it is not a prerequisite for the application of the CPM technique. With the modern fine polishing technique, it is possible to manufacture thin nonlinear crystal sheets down to the ~10 μm level, which has been reported for the frequency doubling of ultrafast lasers [21]. Thus the CPM technique may be adapted to more general cases, that is, the thinner crystal sheet with smaller coherence length and higher Q value. CPM will offer an efficient, high-power solution for nonlinear optical frequency conversion in a thin, monolithic nonlinear device.

In the area of quantum optics, the optical parametric oscillator is widely used to generate squeezing [22] or entanglement [23,24]. As an integrated device, the SOPO features a large optical aperture with single-longitudinal-mode and TEM$_{00}$ output, and therefore, high spectral and spatial brightness nonclassical light can be obtained at both above and below threshold, which is preferred for high fidelity quantum communication and computation.

In our experiment, the SOPO emits near-frequency-degenerate signal and idler beams in pairs, with a quasi-continuously tunable frequency difference ranging from 0.35 to 26.1 THz. By the means of difference frequency generation and simultaneous resonance of signal and idler, terahertz (THz) radiation should exist inside the cavity considerably. In this work, we measured the near infrared output and did not detect the THz signal from the SOPO. In theory, one can roughly estimate THz output to be of tens of milliwatts peak power according to the ~1 MW intra-cavity peak power of signal and idler, under our experimental condition. The study for the generation of effective THz radiation from such a SOPO is under way.

*xiezhenda@smail.nju.edu.cn
†zhusn@nju.edu.cn

[1] S. L. McCall *et al.*, Appl. Phys. Lett. **60**, 289 (1992).
[2] V. S. Ilchenko *et al.*, Phys. Rev. Lett. **92**, 043903 (2004).
[3] J. U. Fürst *et al.*, Phys. Rev. Lett. **104**, 153901 (2010).
[4] T. J. Kippenberg, Physics **3**, 32 (2010).
[5] P. Del'Haye *et al.*, Nature (London) **450**, 1214 (2007).
[6] A. A. Savchenkov *et al.*, Opt. Lett. **32**, 157 (2007).
[7] J. U. Fürst *et al.*, Phys. Rev. Lett. **105**, 263904 (2010).
[8] T. Beckmann *et al.*, arXiv:1012.0801v1.
[9] S. M. Spillane, T. J. Kippenberg, and K. J. Vahala, Nature (London) **415**, 621 (2002).
[10] E. Rosencher, B. Vinter, and V. Berger, J. Appl. Phys. **78**, 6042 (1995).
[11] V. Berger, X. Marcadet, and J. Nagle, Pure Appl. Opt. **7**, 319 (1998).
[12] R. Haïdar, N. Forget, and E. Rosencher, IEEE J. Quantum Electron. **39**, 569 (2003).
[13] J. A. Armstrong *et al.*, Phys. Rev. **127**, 1918 (1962).
[14] D. Feng *et al.*, Appl. Phys. Lett. **37**, 607 (1980).
[15] M. M. Fejer *et al.*, IEEE J. Quantum Electron. **28**, 2631 (1992).
[16] V. Pruneri *et al.*, Appl. Phys. Lett. **67**, 2126 (1995).
[17] S. N. Zhu, Y. Y. Zhu, and N. B. Ming, Science **278**, 843 (1997).
[18] J. E. Schaar, K. L. Vodopyanov, and M. M. Fejer, Opt. Lett. **32**, 1284 (2007).
[19] Y. R. Shen, *The Principles of Nonlinear Optics* (Wiley, New York, 1984).
[20] S. Emanueli and A. Arie, Appl. Opt. **42**, 6661 (2003).
[21] A. Shirakawa *et al.*, Appl. Phys. Lett. **74**, 2268 (1999).
[22] Ling-An Wu *et al.*, Phys. Rev. Lett. **57**, 2520 (1986).
[23] Z. Y. Ou and Y. J. Lu, Phys. Rev. Lett. **83**, 2556 (1999).
[24] X. H. Bao *et al.*, Phys. Rev. Lett. **101**, 190501 (2008).